Early acquisition of S-specific Tfh clonotypes after SARS-CoV-2 vaccination is associated with the longevity of anti-S antibodies

Xiuyuan Lu[1, ¶], Hiroki Hayashi[2, ¶], Eri Ishikawa[1, 3, ¶], Yukiko Takeuchi[1], Julian Vincent Tabora Dychiao[1], Hironori Nakagami[2, *] and Sho Yamasaki[1, 3, 4, *]

[1] Laboratory of Molecular Immunology, Immunology Frontier Research Center, Osaka University, Suita, Osaka, Japan

[2] Department of Health Development and Medicine, Osaka University Graduate School of Medicine, Suita, Osaka, Japan

[3] Department of Molecular Immunology, Research Institute for Microbial Diseases, Osaka University, Suita, Osaka, Japan

[4] Center for Infectious Disease Education and Research (CiDER), Osaka University, Suita, Osaka, Japan

¶These three authors contributed equally to this work.

[*] Co-corresponding authors

Sho Yamasaki: yamasaki@biken.osaka-u.ac.jp

Hironori Nakagami: nakagami@gts.med.osaka-u.ac.jp

Abstract

SARS-CoV-2 vaccines have been used worldwide to combat COVID-19 pandemic. To elucidate the factors that determine the longevity of spike (S)-specific antibodies, we traced the characteristics of S-specific T cell clonotypes together with their epitopes and anti-S antibody titers before and after BNT162b2 vaccination over time. T cell receptor (TCR) αβ sequences and mRNA expression of the S-responded T cells were investigated using single-cell TCR- and RNA-sequencing. Highly expanded 199 TCR clonotypes upon stimulation with S peptide pools were reconstituted into a reporter T cell line for the determination of epitopes and restricting HLAs. Among them, we could determine 78 S epitopes, most of which were conserved in variants of concern (VOCs). In donors exhibiting sustained anti-S antibody titers (designated as "sustainers"), S-reactive T cell clonotypes detected immediately after 2nd vaccination polarized to follicular helper T (Tfh) cells, which was less obvious in "decliners". Even before vaccination, S-reactive $CD4^+$ T cell clonotypes did exist, most of which cross-reacted with environmental or symbiotic bacteria. However, these clonotypes contracted after vaccination. Conversely, S-reactive clonotypes dominated after vaccination were undetectable in pre-vaccinated T cell pool, suggesting that highly-responding S-reactive T cells were established by vaccination from rare clonotypes. These results suggest that *de novo* acquisition of memory Tfh cells upon vaccination contributes to the longevity of anti-S antibody titers.

41 **Introduction**

42 The pandemic COVID-19, caused by the severe acute respiratory syndrome
43 coronavirus 2 (SARS-CoV-2), has expanded worldwide [1]. Many types of vaccines have been
44 developed or in basic and clinical phases to combat infection and deterioration of COVID-19
45 [2,3]. Among them, messenger ribonucleic acid (mRNA) vaccines, BNT162b2/Comirnaty and
46 mRNA-1273/Spikevax, have been approved with over 90% efficacy at 2 months post-2nd dose
47 vaccination [4,5], and widely used. Pathogen-specific antibodies are one of the most efficient
48 components to prevent infection. Yet, mRNA vaccine-induced serum antibody titer is known
49 to be waning over 6 months [6,7]. Accordingly, the effectiveness of the vaccines decreases
50 over time, and thus multiple doses and repeated boosters are necessary [8].

51 The production and sustainability of spike (S)-specific antibody could be related to
52 multiple factors, especially in the case of humans [7,9]. Among them, the characteristics of
53 SARS-CoV-2-specific T cells is critically involved in the affinity and longevity of the
54 antibodies [10–12]. Elucidation of the key factors of T cell responses that contribute to the
55 durable immune responses induced by vaccination would provide valuable information for the
56 vaccine development in the future. However, the relationship between antibody sustainability
57 and the types of antigen-specific T cells has not been investigated in a clonotype resolution.

58 Recent studies reported that S-reactive T cells pre-existed before exposure to SARS-
59 CoV-2 [13–17]. Common cold human coronaviruses (HCoVs) including strains 229E, NL63,
60 OC43, and HKU1 are considered major cross-reactive antigens that primed these pre-existing
61 T cells [15,18–20], while bacterial cross-reactive antigens were also reported [21,22]. However,
62 the functional relevance of cross-reactive T cells during infection or vaccination is still in
63 debate.

64 In this study, both humoral and cellular immune responses were evaluated at 3, 6 and
65 24 weeks after BNT162b2/Comirnaty vaccination. S-specific T cells before and after

66 vaccination were analyzed on clonotype level using single cell-based T cell receptor (TCR)
67 and RNA sequencing to determine their characteristics and epitopes in antibody sustainers and
68 decliners. These analyses suggest the importance of early acquisition of S-specific Tfh cells in
69 the longevity of antibodies.

70 **Results**

71 **SARS-CoV-2 mRNA vaccine elicits transient humoral immunity**

72 Blood samples were collected from a total of 43 individuals (Table 1) who had no
73 SARS-CoV-2 infection history when they received two doses of SARS-CoV-2 mRNA vaccine
74 BNT162b2. Samples were taken before and after the vaccination (Fig. 1A). Consistent with
75 the previous report [4], most participants exhibited more severe side effects after 2nd dose of
76 vaccination than 1st dose locally (Table 2) and systemically (Table 3). At 3 weeks, anti-S IgG
77 antibody titer increased in most participants. At 6 weeks, anti-S antibody titer was at its peak.
78 S antibody titer gradually decreased over 24 weeks (Fig. 1B). The antibody titer was reduced
79 by 56.8% on average. Donors of different genders or age groups showed no significant
80 difference in anti-S antibody titer (Fig. S1). The neutralization activity of the post-vaccinated
81 sera showed similar tendency with the anti-S antibody titer during the study period (Fig. 1C).
82 The above results indicate that the mRNA vaccine effectively activated humoral immune
83 responses in healthy individuals, but decreased by 24 weeks over time as reported [6,7].

84

85 **Antibody sustainers had highly expanded S-reactive Tfh clonotypes**

86 To address the role of T cells in maintaining the antibody titer, we analyzed the S-
87 responsive T cells in the post-vaccination samples from 8 donors, among whom 4 donors
88 showed relatively sustained anti-S antibody titer during 6 weeks to 24 weeks (reduction < 30%)
89 (sustainers, donors #8, #25, #27 and #28), while the other 4 donors showed largely declined
90 anti-S antibody titer (reduction > 80%) (decliners, donors #4, #13, #15 and #17) (Fig. 2A and
91 Fig. S2A). The possibility of SARS-CoV-2 infection of sustainers was ruled out by analyzing
92 anti-nucleocapsid protein (N) antibody titer in the sera samples at 24 weeks (Fig. S2B).
93 Antibody sustainability did not correlate with bulk T cell responses to S protein, such as IFNγ
94 production (Fig. S2C).

95 To enrich the S-reactive T cells, we labeled the peripheral blood mononuclear cells
96 (PBMCs) with a cell proliferation tracer and stimulated the PBMCs with an S peptide pool for
97 10 days. Proliferated T cells were sorted and analyzed by single-cell TCR- and RNA-
98 sequencing (scTCR/RNA-seq). Clustering analysis was done with pooled samples of 3 time
99 points from 8 donors, and various T cell subtypes were identified (Fig. 2B). We found that,
100 overall, the S-reactive T cells did not skew to any particular T cell subset (Fig. 2B). However,
101 by grouping the cells from decliners and sustainers separately, we found difference in the
102 frequency of the cells within the circled population (Fig. 2C). These cells showed high Tfh
103 signature scores and expressed characteristic genes of Tfh cells (Fig. 2D), suggesting that they
104 might be circulating Tfh cells (cTfh) considering they were isolated from PBMCs. This
105 tendency became more pronounced when we selected highly expanded (top 16) clonotypes in
106 each donor (Fig. 2E). In sustainers, S-specific Tfh clusters appeared from 6 weeks (Fig. 2F),
107 suggesting that vaccine-induced Tfh cells were established immediately after 2nd vaccination.
108

109 **Identification of dominant S epitopes recognized by vaccine-induced T cell clonotypes**

110 To elucidate the epitopes of the highly expanded clonotypes, we reconstituted their
111 TCRs into a T cell hybridoma lacking endogenous TCRs and having an NFAT-GFP reporter
112 gene. These cell lines were stimulated with S peptides using transformed autologous B cells as
113 antigen-presenting cells (APCs). The epitopes of 53 out of 128 reconstituted clonotypes were
114 successfully determined (Fig. 3, Table 4, Figs. S3A–S3D). Epitopes of expanded Tfh cells were
115 not limited in any particular region of S protein (Fig. 3). About 72% of these epitopes conserved
116 in Delta and Omicron variants (Tables 4 and 5). Within the rest of 28% of epitopes which were
117 mutated in variants of concerns (VOCs), although some mutated epitopes located in the
118 receptor-binding domain (RBD) of VOCs lost antigenicity, recognition of most epitopes
119 outside the RBD region was maintained or rather increased in the variants (Table 5 and Figs.

120 S3E and S3F). These results suggest that the majority of S-reactive clonotypes after vaccination
121 can respond to antibody-escaping VOCs.
122
123 **Identification of S epitopes and cross-reactive antigens of pre-existing T cell clonotypes**
124 Before the pandemic, T cells cross-reacting to S antigen were present in the peripheral
125 blood [13–17]. To characterize these pre-existing S-reactive cells, we analyzed the PBMCs
126 collected from donors who consented to blood sample donation before vaccination (#4, #8, #13,
127 #15, and #17). PBMCs were stimulated with the S peptide pool for 10 days, and proliferated T
128 cells were sorted and analyzed by scTCR/RNA-seq. Similar to vaccine-induced S-reactive T
129 cells (Fig. 2B), characteristics of pre-existing S-reactive T cells were diverse (Fig. 4A). To
130 track the dynamics of cross-reactive clones after vaccination, we combined the single-cell
131 sequencing data of pre- and post-vaccinated PBMCs and analyzed the clonotypes that have
132 more than 50 cells in total (Fig. 4B). We did find some cross-reactive clonotypes that were
133 further expanded by vaccination, and most of these clonotypes had cytotoxic features, being
134 $CD8^+$ effector memory T cells (Tem) or minor $CD4^+$ cytotoxic T cells (CTLs). In contrast,
135 most of the cross-reactive $CD4^+$ T cells became minor clonotypes after vaccination.
136 We also explored the epitopes of the top 16 expanded clonotypes in each pre-vaccinated
137 donor by reconstituting the TCRs into reporter cell lines. We identified 18 epitopes from S
138 protein (Fig. 5 and Table 6) and determined some possible cross-reactive antigens. Most of
139 these cross-reactive antigens originated from environmental or symbiotic microbes (Table 6).
140 Furthermore, majority of the reactive T clonotypes showed regulatory T cell (Treg) signatures
141 (Fig. 5). Six of these 80 analyzed clonotypes could also be frequently detected in the public
142 TCR database Adaptive [23,24]. Notably, most of these clonotypes, except for one case,
143 showed comparable frequencies between pre-pandemic healthy donors and COVID-19
144 convalescent patients (Fig. 6), suggesting that these clonotypes did not expand upon SARS-

145 CoV-2 infection, despite they were present before the pandemic. Thus, it is unlikely that these
146 cross-reactive T clonotypes contribute to the establishment of S-reactive T cell pools during
147 either vaccination or infection.

148 **Discussion**

149 Previous studies showed that Tfh function and germinal center development were
150 impaired in deceased COVID-19 patients [25] and Tfh cell number correlated with neutralizing
151 antibody [26–28]. Consistent with the above studies, we found that the donors having sustained
152 antibody titers between 6 to 24 weeks post-vaccination had more S antigen-responsive Tfh
153 clonotypes maintained in the periphery as a memory pool. As circulating Tfh clonotypes can
154 reflect the population of germinal center Tfh cells [29], it is possible that these maintained S-
155 responsive Tfh cells contribute to the prolonged production of anti-S antibodies. These results
156 imply that Tfh polarization of S-reactive T cells in the blood after 2nd vaccination can be a
157 marker for the longevity of serum anti-S antibodies. Although monitoring of S-specific Tfh
158 cells in germinal center is ideal [30], it is currently difficult for outpatients in clinics.

159 Since the antigen used for BNT162b2 is a full-length S protein from the Wuhan-Hu-1
160 strain, it is important to estimate whether vaccine-induced Wuhan S-reactive T cells recognize
161 neutralizing antibody-evading VOCs, such as Omicron variants. Consistent with previous
162 reports [31–33], most of the epitopes determined in the current study were conserved in Delta
163 and Omicron (BA.1, BA.2 and BA.4/5) strains, suggesting that vaccine-induced T cells are
164 able to recognize the mutated S proteins from these variants, despite B epitopes being largely
165 mutated in these VOCs [31,32].

166 SARS-CoV-2-recognizing T cells existed prior to exposure of the S antigens [13–17],
167 which is consistent with our observation with PBMCs from donors who were uninfected and
168 pre-vaccinated. Among these pre-existing S-reactive clonotypes, $CD8^+$ cytotoxic T clonotypes
169 were expanded by the vaccination, whereas most of $CD4^+$ T clonotypes became less dominant
170 after vaccination (Fig. 4B). Currently, the reason for the opposite tendency is unclear. In the
171 present study, we showed that pre-existing T clonotypes cross-reacting to S protein are unlikely
172 to contribute to vaccine-driven T cell immunity. This could be due to the fact that cross-reactive

173 T cells had relatively low avidity to S protein [34]. Alternatively, but not mutually exclusively,
174 considering that most of these cross-reactive T clonotypes have Treg signature (Fig. 5), they
175 could be developed to tolerate symbiotic or environmental antigens, and might be ineffective
176 to the defense against SARS-CoV-2 and thus replaced by the other effective T clonotypes
177 induced by vaccination. One exceptional pre-existing clonotype was #15-Pre_2, as they
178 vigorously expanded in COVID-19 patients (Fig. 6). This clonotype was clustered within a
179 $CD4^+$ Tem population and cross-reactive to environmental bacteria, *Myxococcales bacterium*
180 (Table 6). Thus, in some particular settings, clonotypes primed by common bacterial antigens
181 might potentially contribute during infection.

182 Common cold human coronavirus (HCoV)-derived S proteins are reported as potential
183 cross-reactive antigens for pre-existing SARS-CoV-2 S-reactive T cells [15,18–20]. However,
184 the highly responding SARS-CoV-2 S-reactive clonotypes in pre-vaccinated donors rarely
185 reacted with HCoV S proteins in the present study, which might be partly due to the difference
186 of cohorts or ethnicities. Instead, most of those T cells cross-reacted with environmental or
187 symbiotic bacteria. These observations suggest that these cross-reactive T cells might have
188 been developed to establish tolerance against less harmful microbes, and thus unlikely to
189 efficiently contribute to the protective viral immunity. Vaccination may induce opposite
190 tendencies on T cell clonotypes that recognize the same antigen [35], which is hardly detected
191 by the bulk T cell analyses. The current study highlights the necessity of dynamic tracing of T
192 cell responses in an epitope-specific clonotype resolution for the evaluation of vaccine-induced
193 immunity.

194 This study suggests that mRNA vaccine is potent enough to prime rare T cell clonotypes
195 that become dominant afterwards. Furthermore, we propose that the types of $CD4^+$ T
196 clonotypes developed shortly after two doses of vaccination could be an indication of the
197 longevity of antibodies. Tfh-inducing adjuvants or Tfh-skewing epitope would be a promising

198 “directional” booster in the post-vaccine era when most people worldwide were exposed with
199 the same antigen in multiple doses within a short period. Furthermore, in addition to SARS-
200 CoV-2, this strategy can also be applicable for the prevention of other infectious diseases of
201 which neutralizing antibody titers are effective for protection.

202 **Materials and Methods**

203 *Ethics statement and sample collection*

204 This project was approved by Osaka University Institutional Review Board (IRB) (reference
205 No. 21487). 43 volunteers were enrolled in this project. Informed consent was obtained from
206 all participants before the first blood sampling. Samples (serum, whole blood, and PBMCs)
207 were collected four times at 0–7 days before 1st dose vaccination as pre-vaccination, at 14–21
208 days after 1st dose vaccination as 3 weeks sample, at 35–49 days after 1st dose vaccination as
209 6 weeks sample, and at 154–182 days after 1st dose of vaccination as 24 weeks sample. At the
210 same time of blood sampling, adverse event information was also collected from all
211 participants. PBMCs were isolated using BD vacutainer® CPT™ cell separation tube (Beckton
212 Dickinson), according to manufacturers' instructions. Isolated PBMCs were stored in the vapor
213 phase of liquid nitrogen until use.

214

215 *Antibody titer determination by enzyme-linked immunosorbent assay (ELISA)*

216 Serum antibody titer was measured using ELISA. Briefly, recombinant ancestral S protein
217 (S1+S2, Cell Signaling Technology; 1 μg/ml) or recombinant nucleocapsid protein
218 (Acrobiosystems; 1 μg/ml) was coated on 96-well plate at 4 °C overnight. On the second day,
219 wells were blocked with blocking buffer (PBS-T (0.05% tween®20) containing 5% skim milk)
220 for 2 h at room temperature. The sera were diluted from 10 to 31,250 folds in blocking buffer
221 and incubated overnight at 4 °C. The next day, wells were washed and incubated with
222 horseradish peroxidase (HRP)-conjugated antibodies (GE Healthcare) for 3 h at room
223 temperature. After being washed with PBS-T, wells were incubated with the peroxidase
224 chromogenic substrate 3,3'-5,5'-tetramethyl benzidine (Sigma-Aldrich) for 30 min at room
225 temperature, then the reaction was stopped by 0.5 N sulfuric acid (Sigma Aldrich). The
226 absorbance of wells was immediately measured at 450 nm with a microplate reader (Bio-Rad).

227 The value of the half-maximal antibody titer of each sample was calculated from the highest
228 absorbance in the dilution range by using Prism 8 software. The calculated antibody titer was
229 converted to BAU/ml by using WHO International Standard 20/136 (NIBSC) for ancestral S-
230 specific antibody titer.
231
232 *Whole blood interferon-gamma release immune assay (IGRA) for SARS-CoV-2 specific T cell*
233 *responses using QuantiFERON*
234 SARS-CoV-2 specific T cell immune responses were evaluated by QuantiFERON SARS-
235 CoV-2 (Qiagen) [36], according to manufacturer's instructions, in which $CD4^+$ T cells were
236 activated by epitopes coated on Ag1 tube, and $CD4^+$ and $CD8^+$ T cells were activated by
237 epitopes coated on Ag2 tube. Briefly, 1 ml of whole blood sample with heparin is added into
238 each of Nil (negative control), Mito (positive control), Ag1, and Ag2 tubes, and incubated at
239 37 °C for 22–24 h. Tubes were then centrifuged at 3,000 × g for 15 min for collecting plasma
240 samples. IFNγ derived from activated T cells was measured with enzyme-linked
241 immunosorbent assay (ELISA) (Qiangen) according to the manufacturer's instructions. IFNγ
242 concentration (IU/ml) was calculated with background (Nil tube) subtracted from values of
243 Ag1 or Ag2 tubes.
244
245 *Pseudo-typed virus neutralization assay*
246 The neutralizing activity of serum antibodies was analyzed with pseudo-typed VSVs as
247 previously described [37]. Briefly, Vero E6 cells stably expressing TMPRSS2 were seeded on
248 96-well plates and incubated at 37 °C for 24 h. Pseudoviruses were incubated with a series of
249 dilutions of inactivated serum for 1 h at 37 °C, then added to Vero E6 cells. At 24 h after
250 infection, cells were lysed with cell culture lysis reagent (Promega), and luciferase activity was
251 measured by Centro XS^3 LB 960 (Berthold).

252

253 *In vitro stimulation of PBMCs*

254 Cryopreserved PBMCs were thawed and washed with warm RPMI 1640 medium (Sigma)
255 supplemented with 5% human AB serum (GeminiBio), Penicillin (Sigma), streptomycin (MP
256 Biomedicals), and 2-mercaptoethanol (Nacalai Tesque). PBMCs were labeled with Cell
257 Proliferation Kit (CellTrace™ Violet, ThermoFisher) following the manufacturer's protocol
258 and were stimulated in the same medium with S peptide pool (1 μg/ml per peptide, JPT) for 10
259 days, with human recombinant IL-2 (1 ng/ml, Peprotech), IL-7 (5 ng/ml, BioLegend) and IL-
260 15 (5 ng/ml, Peprotech) supplemented on day 2, day 5 and day 8 of the culture. On day 10 cells
261 were washed and stained with anti-human CD3 and TotalSeq-C Hashtags antibodies.
262 Proliferated T cells ($CD3^{+}CTV^{low}$) were sorted by cell sorter SH800S (SONY) and used for
263 single-cell TCR and RNA sequencing analyses.

264

265 *Single cell-based transcriptome and TCR repertoire analysis*

266 Single cell library was prepared using the reagents from 10x Genomics following the
267 manufacturer's instructions. After reverse transcription, cDNA was amplified for 14 cycles,
268 and up to 50 ng of cDNA was used for construction of gene expression and TCR libraries.
269 Libraries were sequenced in paired-end mode, and the raw reads were processed by Cell Ranger
270 3.1.0 (10x Genomics). Doublets and empty drops were removed by using Scrublet [38] and
271 gating out the events whose main hashtag reads are less than 95% of the total hashtag reads.
272 The top 4000 highly variable genes were used for clustering. Tfh signature score was generated
273 using canonical Tfh marker genes (*IL21*, *ICOS*, *CD200, PDCD1*, *POU2AF1*, *BTLA*, *CXCR5,*
274 and *CXCL13*) and UMAP plots were exported using BBrowser [39].

275

276 *Reporter cell establishment and stimulation*

277 TCRα and β chain cDNA sequences were introduced into a mouse T cell hybridoma lacking
278 TCR and having a nuclear factor of activated T-cells (NFAT)-green fluorescent protein (GFP)
279 reporter gene [40] using retroviral vectors. TCR-reconstituted cells were co-cultured with 1
280 μg/ml of peptides in the presence of antigen-presenting cells (APCs). After 20 h, cell activation
281 was assessed by GFP and CD69 expression.
282
283 *Antigen-presenting cells*
284 Transformed B cells and HLA-transfected HEK293T cells used as APCs were generated as
285 described [21]. For transformed B cells, 3×10^5 PBMCs were incubated with the recombinant
286 Epstein-Barr virus (EBV) suspension [41] for 1 h at 37°C with mild shaking every 15 min. The
287 infected cells were cultured in RPMI 1640 medium supplemented with 20% fetal bovine serum
288 (FBS, CAPRICORN SCIENTIFIC GmbH) containing cyclosporine A (CsA, 0.1 μg/ml,
289 Cayman Chemical). Immortalized B lymphoblastoid cell lines were obtained after 3 weeks of
290 culture and used as APCs. For HLA-transfected HEK293T cells, plasmids encoding HLA class
291 I/II alleles [42] were transfected in HEK293T cells with PEI MAX (Polysciences).
292
293 *Determination of epitopes and restricting HLA*
294 15-mer peptides with 11 amino acids overlap that cover the full length of S protein of SARS-
295 CoV-2 were synthesized (GenScript). Peptides were dissolved in DMSO at 12 mg/ml and 12-
296 15 peptides were mixed to create 26 different semi-pools. TCR-reconstituted reporter cells
297 were stimulated with 1 μg/ml of S peptide pool (1 μg/ml per peptide, JPT), then 36-peptide
298 pools that consist of 3 semi-pools each, then semi-pools, and then 12 individual peptides in the
299 presence of autologous B cells to identify epitope peptides. To determine the restricting HLA,
300 HLAs were narrowed down by co-culturing reporter cells with autologous and various
301 heterologous B cells in the presence of 1 μg/ml of the epitope peptide. HLAs shared by

302 activatable B cells were transduced in HEK239T cells and used for further co-culture to
303 identify the restricting HLA.
304
305 *Statistics*
306 All values with error bars are presented as the mean ± SEM. One-way ANOVA followed by
307 Turkey's post hoc multiple comparison test was used to assess significant differences in each
308 experiment using Prism 8 software (GraphPad Software). Differences were considered to be
309 significant when *P* value was less than 0.05. *P* values in Fig. 6 were calculated with t-test using
310 the "stat_compare_means" function in R.

Acknowledgements

We thank S. Iwai, Y. Sakai, C. Günther, J. Sun, and Y. Yanagida for experimental support, D. Motooka, D. Okuzaki, and YC. Liu for bioinformatic data analysis and C. Schutt and Y. Yamagishi for discussion. This research was supported by Japan Agency for Medical Research and Development (JP223fa627002, JP223fa727001, JP23ym0126049 (SY), JP21ym0126049 (HN)) and Japan Society for the Promotion of Science Grants-in-Aid for Scientific Research (JP20H00505, JP22H05182, JP22H05183 (SY)). The Department of Health Development and Medicine is an endowed department supported by AnGes, Daicel, and FunPep.

References

1. Hu B, Guo H, Zhou P, Shi ZL. Characteristics of SARS-CoV-2 and COVID-19. Nature Reviews Microbiology 2020 19:3. 2021;19: 141–154. doi:10.1038/s41579-020-00459-7
2. Krammer F. SARS-CoV-2 vaccines in development. Nature. 2020;586: 516–527. doi:10.1038/s41586-020-2798-3
3. Creech CB, Walker SC, Samuels RJ. SARS-CoV-2 Vaccines. JAMA. 2021;325: 1318–1320. doi:10.1001/JAMA.2021.3199
4. Polack FP, Thomas SJ, Kitchin N, Absalon J, Gurtman A, Lockhart S, et al. Safety and Efficacy of the BNT162b2 mRNA Covid-19 Vaccine. New England Journal of Medicine. 2020;383: 2603–2615. doi:10.1056/NEJMOA2034577
5. Baden LR, el Sahly HM, Essink B, Kotloff K, Frey S, Novak R, et al. Efficacy and Safety of the mRNA-1273 SARS-CoV-2 Vaccine. New England Journal of Medicine. 2021;384: 403–416. doi:10.1056/nejmoa2035389
6. Pegu A, O'Connell SE, Schmidt SD, O'Dell S, Talana CA, Lai L, et al. Durability of mRNA-1273 vaccine-induced antibodies against SARS-CoV-2 variants. Science. 2021;373: 1372–1377. doi:10.1126/SCIENCE.ABJ4176
7. Levin EG, Lustig Y, Cohen C, Fluss R, Indenbaum V, Amit S, et al. Waning Immune Humoral Response to BNT162b2 Covid-19 Vaccine over 6 Months. New England Journal of Medicine. 2021;385: e84. doi:10.1056/NEJMOA2114583
8. Andrews N, Stowe J, Kirsebom F, Toffa S, Rickeard T, Gallagher E, et al. Covid-19 Vaccine Effectiveness against the Omicron (B.1.1.529) Variant. New England Journal of Medicine. 2022;386: 1532–1546. doi:10.1056/NEJMoa2119451
9. Collier DA, de Marco A, Ferreira IATM, Meng B, Datir RP, Walls AC, et al. Sensitivity of SARS-CoV-2 B.1.1.7 to mRNA vaccine-elicited antibodies. Gabriela Barcenas-Morales. 2021;593: 136. doi:10.1038/s41586-021-03412-7
10. Nelson RW, Chen Y, Venezia OL, Majerus RM, Shin DS, Carrington MN, et al. SARS-CoV-2 epitope–specific CD4+ memory T cell responses across COVID-19 disease severity and antibody durability. Sci Immunol. 2022;7: 9464. doi:10.1126/SCIIMMUNOL.ABL9464
11. Terahara K, Sato T, Adachi Y, Tonouchi K, Onodera T, Moriyama S, et al. SARS-CoV-2-specific CD4+ T cell longevity correlates with Th17-like phenotype. iScience. 2022;25: 104959. doi:10.1016/J.ISCI.2022.104959
12. Crotty S. T Follicular Helper Cell Biology: A Decade of Discovery and Diseases. Immunity. 2019;50: 1132–1148. doi:10.1016/j.immuni.2019.04.011
13. Grifoni A, Weiskopf D, Ramirez SI, Mateus J, Dan JM, Moderbacher CR, et al. Targets of T Cell Responses to SARS-CoV-2 Coronavirus in Humans with COVID-19 Disease and Unexposed Individuals. Cell. 2020;181: 1489-1501.e15. doi:10.1016/j.cell.2020.05.015
14. Meckiff BJ, Ramírez-Suástegui C, Fajardo V, Chee SJ, Kusnadi A, Simon H, et al. Imbalance of Regulatory and Cytotoxic SARS-CoV-2-Reactive CD4+ T Cells in COVID-19. Cell. 2020; 1–14. doi:10.1016/j.cell.2020.10.001
15. Mateus J, Grifoni A, Tarke A, Sidney J, Ramirez SI, Dan JM, et al. Selective and cross-reactive SARS-CoV-2 T cell epitopes in unexposed humans. Science. 2020;370: 89–94. doi:10.1126/science.abd3871
16. Sekine T, Perez-Potti A, Rivera-Ballesteros O, Strålin K, Gorin JB, Olsson A, et al. Robust T Cell Immunity in Convalescent Individuals with Asymptomatic or Mild COVID-19. Cell. 2020;183: 158-168.e14. doi:10.1016/j.cell.2020.08.017

17. le Bert N, Tan AT, Kunasegaran K, Tham CYL, Hafezi M, Chia A, et al. SARS-CoV-2-specific T cell immunity in cases of COVID-19 and SARS, and uninfected controls. Nature. 2020;584: 457–462. doi:10.1038/s41586-020-2550-z
18. Loyal L, Braun J, Henze L, Kruse B, Dingeldey M, Reimer U, et al. Cross-reactive CD4+ T cells enhance SARS-CoV-2 immune responses upon infection and vaccination. Science. 2021;374. doi:10.1126/science.abh1823
19. Low JS, Vaqueirinho D, Mele F, Foglierini M, Jerak J, Perotti M, et al. Clonal analysis of immunodominance and crossreactivity of the CD4 T cell response to SARS-CoV-2. Science. 2021;372: 1336–1341. doi:10.1126/science.abg8985
20. Becerra-Artiles A, Calvo-Calle JM, Co MD, Nanaware PP, Cruz J, Weaver GC, et al. Broadly recognized, cross-reactive SARS-CoV-2 CD4 T cell epitopes are highly conserved across human coronaviruses and presented by common HLA alleles. Cell Rep. 2022;39: 110952. doi:10.1016/J.CELREP.2022.110952
21. Lu X, Hosono Y, Nagae M, Ishizuka S, Ishikawa E, Motooka D, et al. Identification of conserved SARS-CoV-2 spike epitopes that expand public cTfh clonotypes in mild COVID-19 patients. Journal of Experimental Medicine. 2021;218. doi:10.1084/jem.20211327
22. Bartolo L, Afroz S, Pan Y-G, Xu R, Williams L, Lin C-F, et al. SARS-CoV-2-specific T cells in unexposed adults display broad trafficking potential and cross-react with commensal antigens. Sci Immunol. 2022;7. doi:10.1126/sciimmunol.abn3127
23. Emerson RO, DeWitt WS, Vignali M, Gravley J, Hu JK, Osborne EJ, et al. Immunosequencing identifies signatures of cytomegalovirus exposure history and HLA-mediated effects on the T cell repertoire. Nat Genet. 2017;49: 659–665. doi:10.1038/ng.3822
24. Nolan S, Vignali M, Klinger M, Dines JN, Kaplan IM, Craft T, et al. A large-scale database of T-cell receptor beta (TCR β) sequences and binding associations from natural and synthetic exposure to SARS-CoV-2. Res Sq. 2020; 10.21203/RS.3.RS-51964/V1. doi:10.21203/RS.3.RS-51964/V1
25. Kaneko N, Kuo HH, Boucau J, Farmer JR, Allard-Chamard H, Mahajan VS, et al. Loss of Bcl-6-Expressing T Follicular Helper Cells and Germinal Centers in COVID-19. Cell. 2020;183: 143-157.e13. doi:10.1016/j.cell.2020.08.025
26. Gong F, Dai Y, Zheng T, Cheng L, Zhao D, Wang H, et al. Peripheral CD4+ T cell subsets and antibody response in COVID-19 convalescent individuals. Journal of Clinical Investigation. 2020;130: 6588–6599. doi:10.1172/JCI141054
27. Juno JA, Tan HX, Lee WS, Reynaldi A, Kelly HG, Wragg K, et al. Humoral and circulating follicular helper T cell responses in recovered patients with COVID-19. Nat Med. 2020;26: 1428–1434. doi:10.1038/s41591-020-0995-0
28. Zhang J, Wu Q, Liu Z, Wang Q, Wu J, Hu Y, et al. Spike-specific circulating T follicular helper cell and cross-neutralizing antibody responses in COVID-19-convalescent individuals. Nature Microbiology 2020 6:1. 2021;6: 51–58. doi:10.1038/s41564-020-00824-5
29. Brenna E, Davydov AN, Ladell K, McLaren JE, Bonaiuti P, Metsger M, et al. CD4 + T Follicular Helper Cells in Human Tonsils and Blood Are Clonally Convergent but Divergent from Non-Tfh CD4 + Cells. Cell Rep. 2020;30: 137-152.e5. doi:10.1016/J.CELREP.2019.12.016
30. Mudd PA, Minervina AA, Pogorelyy M v., Turner JS, Kim W, Kalaidina E, et al. SARS-CoV-2 mRNA vaccination elicits a robust and persistent T follicular helper cell response in humans. Cell. 2022;185: 603-613.e15. doi:10.1016/J.CELL.2021.12.026

31. Tarke A, Coelho CH, Zhang Z, Dan JM, Yu ED, Methot N, et al. SARS-CoV-2 vaccination induces immunological T cell memory able to cross-recognize variants from Alpha to Omicron. Cell. 2022;185: 847-859.e11. doi:10.1016/J.CELL.2022.01.015
32. GeurtsvanKessel CH, Geers D, Schmitz KS, Mykytyn AZ, Lamers MM, Bogers S, et al. Divergent SARS-CoV-2 Omicron–reactive T and B cell responses in COVID-19 vaccine recipients. Sci Immunol. 2022;7: eabo2202. doi:10.1126/sciimmunol.abo2202
33. Keeton R, Tincho MB, Ngomti A, Baguma R, Benede N, Suzuki A, et al. T cell responses to SARS-CoV-2 spike cross-recognize Omicron. Nature. 2022;603: 488–492. doi:10.1038/s41586-022-04460-3
34. Bacher P, Rosati E, Esser D, Martini GR, Saggau C, Schiminsky E, et al. Low-Avidity CD4+ T Cell Responses to SARS-CoV-2 in Unexposed Individuals and Humans with Severe COVID-19. Immunity. 2020;53: 1258-1271.e5. doi:10.1016/j.immuni.2020.11.016
35. Aoki H, Kitabatake M, Abe H, Shichino S, Hara A, Ouji-Sageshima N, et al. T cell responses induced by SARS-CoV-2 mRNA vaccination are associated with clonal replacement. bioRxiv. 2022; 2022.08.27.504955. doi:10.1101/2022.08.27.504955
36. Jaganathan S, Stieber F, Rao SN, Nikolayevskyy V, Manissero D, Allen N, et al. Preliminary Evaluation of QuantiFERON SARS-CoV-2 and QIAreach Anti-SARS-CoV-2 Total Test in Recently Vaccinated Individuals. Infect Dis Ther. 2021;10: 2765–2776. doi:10.1007/S40121-021-00521-8
37. Yoshida S, Ono C, Hayashi H, Fukumoto S, Shiraishi S, Tomono K, et al. SARS-CoV-2-induced humoral immunity through B cell epitope analysis in COVID-19 infected individuals. Scientific Reports 2021 11:1. 2021;11: 1–13. doi:10.1038/s41598-021-85202-9
38. Wolock SL, Lopez R, Klein AM. Scrublet: Computational Identification of Cell Doublets in Single-Cell Transcriptomic Data. Cell Syst. 2019;8: 281-291.e9. doi:10.1016/J.CELS.2018.11.005
39. Le T, Phan T, Pham M, Tran D, Lam L, Nguyen T, et al. BBrowser: Making single-cell data easily accessible. bioRxiv. 2020; 2020.12.11.414136. doi:10.1101/2020.12.11.414136
40. Matsumoto Y, Kishida K, Matsumoto M, Matsuoka S, Kohyama M, Suenaga T, et al. A TCR-like antibody against a proinsulin-containing fusion peptide ameliorates type 1 diabetes in NOD mice. Biochem Biophys Res Commun. 2021;534: 680–686. doi:10.1016/j.bbrc.2020.11.019
41. Kanda T, Miyata M, Kano M, Kondo S, Yoshizaki T, Iizasa H. Clustered MicroRNAs of the Epstein-Barr Virus Cooperatively Downregulate an Epithelial Cell-Specific Metastasis Suppressor. J Virol. 2015;89: 2684–2697. doi:10.1128/jvi.03189-14
42. Jiang Y, Arase N, Kohyama M, Hirayasu K, Suenaga T, Jin H, et al. Transport of misfolded endoplasmic reticulum proteins to the cell surface by MHC class II molecules. Int Immunol. 2013;25: 235–246. doi:10.1093/intimm/dxs155

Tables

Table 1. Demographic data of the participants.

	Percentage (number)
Total number	100% (43)
Age group	
20-39	39.5% (17)
40-49	30.2% (13)
50-59	25.6% (11)
60-69	4.7% (2)
Gender	
Male	60.5% (26)
Female	39.5% (17)

Table 2. Demographic data of the reported clinical adverse effects (at injection site)

	Percentage (number)
Swelling (injection site)	
After 1st dose	27.9% (12)
After 2nd dose	51.2% (22)
Sore/pain (injection site)	
After 1st dose	88.4% (38)
After 2nd dose	86.0% (37)
Warmth (injection site)	
After 1st dose	32.6% (14)
After 2nd dose	41.9% (18)

Table 3. Demographic data of the reported clinical adverse effects (systemic symptoms)

	Percentage (number)
Fever	
After 1st dose	
Mild (37.5°C ≥)	2.3% (1)
Severe (≥ 38.0°C)	0% (0)
After 2nd dose	
Mild (37.5°C ≥)	25.6% (11)
Severe (≥ 38.0°C)	23.3% (10)
Fatigue	
After 1st dose	
Mild	18.6% (8)
Severe	0% (0)
After 2nd dose	
Mild	67.4% (29)
Severe	18.6% (8)
Headache	
After 1st dose	
Mild	7.0% (3)
Severe	0% (0)
After 2nd dose	
Mild	32.6% (14)
Severe	7.0% (3)
Chill	
After 1st dose	
Mild	4.7% (2)
Severe	0% (0)
After 2nd dose	
Mild	23.3% (10)
Severe	9.3% (4)
Nausea	
After 1st dose	
Mild	0% (0)
Severe	0% (0)
After 2nd dose	
Mild	4.7% (2)
Severe	0% (0)
Diarrhea	
After 1st dose	
Mild	0% (0)
Severe	0% (0)
After 2nd dose	
Mild	0% (0)
Severe	0% (0)
Muscle pain	
After 1st dose	
Mild	48.8% (21)
Severe	0% (0)
After 2nd dose	
Mild	55.8% (24)
Severe	4.7% (2)
Joint pain	
After 1st dose	
Mild	4.7% (2)
Severe	0% (0)
After 2nd dose	
Mild	25.6% (11)
Severe	4.7% (2)

Table 4. TCR clonotypes expanded in post-vaccinated samples and their TCR usages, epitopes and restricting HLAs.

Donor	Clonotype	TRBV	CDR3β	TRBJ	TRAV	CDR3α	TRAJ	S epitope[a]	Restricting HLA
#8	Post_4	11-2	CASSPTGTNEKLFF	1-4	13-1	CAGGADGLTF	45	SFSTFKCYGVSPTKL$_{373–387}$[b]	DRA-DRB1*15:02
	Post_5	19	CASSGRPEGPQHF	1-5	20	CAVLNQAGTALIF	15	FKIYSKHTPIN$_{201–211}$	DRA-DRB1*09:01
	Post_6	11-2	CASSLEGTEAFF	1-1	5	CAESRYMGRRALTF	5	FQFCNDPFLGVYYHK$_{133–147}$	DPA1*01:03-DPB1*04:02
	Post_7	2	CAGLAGVDTGELFF	2-2	5	CAERVGRRALTF	5	YSVLYNSASFSTFKC$_{365–379}$	A*24:02
	Post_8	20-1	CSATRDRRSYNEQFF	2-1	12-2	CAVLTNTGNQFYF	49	LLQYGSFCTQLNRAL$_{753–767}$	DRA-DRB1*15:02
	Post_9	7-9	CASSLLGEQYF	2-7	22	CAGAGGTSYGKLTF	52	KRFDNPVLPFN$_{77–87}$	DPA1*02:02-DPB1*05:01
	Post_10	6-1	CASSEGASNQPQHF	1-5	12-1	CVVNKGSSASKIIF	3	LLQYGSFCTQL$_{753–763}$	DRA-DRB1*15:02
	Post_12	20-1	CSAYSIYNEQFF	2-1	9-2	CALSMNTGFQKLVF	8	PPAYTNSFTRGVYYP$_{25–39}$	DRA-DRB1*09:01
	Post_14	19	CASRPNRGDNSPLHF	1-6	12-1	CVVSIGFGNVLHC	35	CSNLLLQYGSFCTQL$_{749–763}$	DRA-DRB1*15:02
	Post_15	28	CASSLMGGAYGYTF	1-2	8-6	CAVRRGGSGGSNYKLTF	53	SKRSFIEDLLFNKVT$_{813–827}$	DPA1*01:03-DPB1*04:02
#25	Post_7	7-9	CAPSNANTGELFF	2-2	12-1	CVVNEADKLIF	34	YLQPRTFLLK$_{269–278}$	A*02:01
	Post_12	20-1	CSARDVEVGSGYTF	1-2	4	CLVGPYNQGGKLIF	23	TGVLTESNKKFLPFQ$_{549–563}$	DRA-DRB1*14:54
	Post_15	3-1	CASSPLSGSSYEQYF	2-7	12-1	CVVGTDSWGKLQF	24	TNGTKRFDNPVLPFN$_{73–87}$	DPA1*02:02-DPB1*05:01/ DPA1*01:03-DPB1*05:01
#27	Post_1	20-1	CSAIAGDADTQYF	2-3	9-2	CALTSAAGNKLTF	17	NQFNSAIGKIQ$_{925–935}$	DRA-DRB1*09:01
	Post_2	30	CAWNLGGGNQPQHF	1-5	8-2	CVVSERASSYKLIF	12	SKRSFIEDLLFNKVT$_{813–827}$	DPA1*02:02-DPB1*04:02
	Post_3	5-4	CASSQGQGSYGYTF	1-2	4	CLVGDSDTGRRALTF	5	NFTISVTTEIL$_{717–727}$	DRA-DRB1*09:01
	Post_5	7-2	CASGTGSYNEQFF	2-1	12-2	CAVKRGNQGGKLIF	23	STEIYQAGSTPCNGV$_{469–483}$	DRA-DRB1*04:03
	Post_7	6-6	CASRLPGNRAQPQHF	1-5	36/DV7	CAVESGSSNTGKLIF	37	KSNIIRGWIFGTTLD$_{97–111}$	DRA-DRB4*01:03
	Post_8	6-5	CASSYSGGTVTGELFF	2-2	41	CAVGIRGNEKLTF	48	KVFRSSVLHST$_{41–51}$	DRA-DRB1*04:03
	Post_9	20-1	CSARDGQTATNEKLFF	1-4	17	CATNAGGTSYGKLTF	52	EIRASANLAAT$_{1017–1027}$	DRA-DRB1*04:03
	Post_11	30	CAWSVKGFPSQHF	1-5	6	CALGSTSNTGKLIF	37	EIRASANLAAT$_{1017–1027}$	DRA-DRB1*04:03
	Post_13	5-6	CASSSRTGYNSPLHF	1-6	27	CAGAKGSGTYKYIF	40	STEIYQAGSTPCNGV$_{469–483}$	DRA-DRB1*04:03
	Post_15	5-5	CASSSDRNYGYTF	1-2	12-1	CVVNMVTGGYNKLIF	4	NFTISVTTEILPVSM$_{717–731}$	DRA-DRB1*09:01
	Post_16	7-9	CASSSQPGLAGVKIGNEQFF	2-1	5	CAEIPPPSNTGKLIF	37	ISGINASVVNIQKEI$_{1169–1183}$	DRA-DRB1*04:03
#28	Post_5	3-1	CASSQGGSEKLFF	1-4	1-1	CAVGGNTDKLIF	34	LVKNKCVNFNF$_{533–543}$	DRA-DRB3*03:01
	Post_10	12-3	CASSSGRTGFGYTF	1-2	30	CGTEFGSEKLVF	57	VIRGDEVRQIA$_{401–411}$	DRA-DRB3*03:01
	Post_11	5-8	CASSLQKTTGPSYGYTF	1-2	8-6	CAVSPYTGRRALTF	5	SVYAWNRKRIS$_{349–359}$	DRA-DRB1*13:02
	Post_12	18	CASSASVDPTEAFF	1-1	1-1	CASFTGGGNKLTF	10	KSTNLVKNKCVNFNF$_{529–543}$	DRA-DRB3*03:01
	Post_14	7-6	CASSLSGTGGTGELFF	2-2	4	CLVGDMRSGGGADGLTF	45	PFGEVFNATRFASVY$_{337–351}$	B*40:01
	Post_15	6-2	CASSYPPSGGRTGFGEAFF	1-1	14/DV4	CAMRDIGFGNVLHC	35	WNRKRISNCVADYSV$_{353–367}$	DRA-DRB4*01:03

[a]Overlapped epitope sequence is shown when a clonotype recognized two or three sequential peptides.
[b]Number ranges indicate the location of peptides in the proteins.

Table 4. Continued.

Donor	Clonotype	TRBV	CDR3β	TRBJ	TRAV	CDR3α	TRAJ	S epitope	Restricting HLA
#4	Post_2	25-1	CASTGDNYGYTF	1-2	21	CAINTGNQFYF	49	YYVGYLQPR$_{265–273}$	A*33:03
	Post_10	7-9	CASRPSGTSREQYF	2-7	29	CAGNNAGNMLTF	39	FIKQYGDCLGDIAAR$_{833–847}$	A*33:03
	Post_11	7-9	CASSTRTSGGGLSYEQYF	2-7	3	CAVNKAAGNKLTF	17	YSVLYNSASFSTFKC$_{365–379}$	A*24:02
	Post_13	20-1	CSASIEQGDLGYTF	1-2	23/DV6	CAASIPNSGYALNF	41	FIKQYGDCLGDIAAR$_{833–847}$	DQA1*01:02-DQB1*05:03
	Post_14	5-6	CASSPGQGILEQYF	2-7	24	CAFVPLSDGQKLLF	16	YIKWPWYIWL$_{1209–1218}$	A*24:02
	Post_15	7-3	CASGIHTGELFF	2-2	26-1	CIVNNAGNMLTF	39	TDNTFVSGNCDVVIG$_{1117–1131}$	DQA1*01:02-DQB1*06:04
	Post_16	7-6	CASSPGPSEADTQYF	2-3	1-1	CAVRDGDDKIIF	30	KSTNLVKNKCVNFNF$_{529–543}$	DRA-DRB3*03:01
#13	Post_13	7-2	CASSVGQSKGKSAETQYF	2-5	22	CAVNEYSGAGSYQLTF	28	SKRSFIEDLLFNKVT$_{813–827}$	DPA1*01:03-DPB1*02:01
	Post_15	20-1	CSAGDTASTYGYTF	1-2	9-2	CALSDGAGNKLTF	17	NQFNSAIGKIQ$_{925–935}$	DRA-DRB1*09:01
	Post_16	30	CAWSLQGQRPQHF	1-5	38-1	CAFMKQRGGSEKLVF	57	FIEDLLFNKVTLADA$_{817–831}$	DPA1*01:03-DPB1*02:01
#15	Post_1	12-4	CASSSHRDRGVEAFF	1-1	12-1	CVVNFDRGSTLGRLYF	18	TRGVYYPDKVF$_{33–43}$	B*15:01
	Post_6	3-1	CASSQQLNTGELFF	2-2	38-2/DV8	CAYRKTSGTYKYIF	40	WRVYSTGSNVF$_{633–643}$	DRA-DRB1*15:02
	Post_7	28	CASSFPDRYYSNQPQHF	1-5	1-2	CAVRAVGGNKLVF	47	TRGVYYPDKVF$_{33–43}$	B*15:01
	Post_9	27	CASSPGHEQYF	2-7	14/DV4	CAMSPIRTYKYIF	40	RSVASQSIIAY$_{685–695}$	B*15:01
	Post_11	3-1	CASSRELISEQYF	2-7	38-2/DV8	CAYKRTSGTYKYIF	40	WRVYSTGSNVF$_{633–643}$	DRA-DRB1*15:02
	Post_12	28	CASSSYGTSGGRAEQFF	2-1	16	CALSGGLTGGGNKLTF	10	LGDIAARDLICAQKF$_{841–855}$	DRA-DRB1*08:02
	Post_13	30	CAWRTGQGITSPLHF	1-6	8-2	CVVNNAGNMLTF	39	VFKNIDGYFKIYSKH$_{193–207}$	DPA1*02:02-DPB1*05:01
	Post_14	6-1	CASSEAGGSGANVLTF	2-6	9-2	CALSGTGTYKYIF	40	KKFLPFQQFGR$_{557–567}$	DPA1*02:02-DPB1*05:01
	Post_16	27	CASSLGTINTGELFF	2-2	17	CATAPAGGTSYGKLTF	52	IDGYFKIYSKHTPIN$_{197–211}$	DRA-DRB1*08:02
#17	Post_4	6-2	CASTSTARGSYNEQFF	2-1	27	CAGHSNTGNQFYF	49	TRFASVYAWNRKRIS$_{345–359}$	DRA-DRB1*08:02
	Post_10	9	CASSKTSGAYNEQFF	2-1	9-2	CALDNARLMF	31	FIKQYGD$_{833–839}$	DRA-DRB1*15:01
	Post_11	20-1	CSARPPGGGNNEQFF	2-1	26-2	CILRDGTGANNLFF	36	QALNTLVKQLSSNFG$_{957–971}$	DRA-DRB1*08:02
	Post_15	7-9	CASSLARGNSPLHF	1-6	38-2/DV8	CAFVGSQGNLIF	42	AARDLICAQKFNGLT$_{845–859}$	DRA-DRB1*08:02

Table 5. Reactivity of each clonotype to mutated epitopes in SARS-CoV-2 VOCs.

Donor	Clonotype	Mutated epitopes in VOCs		Domain	Response
#8	Post_4	Omicron BA.1 Omicron BA.2, 4/5	PFFTFKCYGVSPTKL[a] PFFAFKCYGVSPTKL	RBD	↓ ↓
#8	Post_5	Omicron BA.1	FKIYSKHTPII	non-RBD	↑
#8	Post_6	Delta, Omicron BA.2, 4/5 Omicron BA.1	FQFCNDPFLDVYYHK FQFCNDPFLD---HK	non-RBD	↓ ↓
#8	Post_7	Omicron BA.1 Omicron BA.2, 4/5	YSVLYNLAPFFTFKC YSVLYNFAPFFAFKC	RBD	↓ ↓
#8	Post_8	Omicron BA1, 2, 4/5	LLQYGSFCTQLKRAL	non-RBD	↑
#8	Post_10	Omicron BA1, 2, 4/5	LLQYGSFCTQLKRAL	non-RBD	↑
#27	Post_5	Delta Omicron BA.1, 2, 4/5	STEIYQAGSKPCNGV STEIYQAGNKPCNGV	RBD	↓ ↓
#27	Post_13	Delta Omicron BA.1, 2, 4/5	STEIYQAGSKPCNGV STEIYQAGNKPCNGV	RBD	↓ ↓
#28	Post_5	Omicron BA.1	LVKNKCVNFNFNGLK	non-RBD	↑
#28	Post_10	Omicron BA.2, 4/5	VIRGNEVSQIA	RBD	↓
#28	Post_14	Omicron BA.1, 2, 4/5	PFDEVFNATRFASVY	RBD	↓
#4	Post_11	Omicron BA.1 Omicron BA.2, 4/5	YSVLYNLAPFFTFKC YSVLYNFAPFFAFKC	RBD	↓ ↓
#15	Post_9	Delta Omicron BA.1, 2, 4/5	RRRARSVASQSIIAY HRRARSVASQSIIAY	non-RBD	↑ ↑
#15	Post_16	Omicron BA.1	IDGYFKIYSKHTPII	non-RBD	→
#17	Post_11	Omicron BA.1, 2, 4/5	QALNTLVKQLSSKFG	non-RBD	↓
#17	Post_15	Omicron BA.1	AARDLICAQKFKGLT	non-RBD	↓

[a]Amino acids colored red indicate mismatches compared with corresponding S epitopes of Wuhan strain.

Table 6. S-cross-reactive TCR clonotypes expanded in pre-vaccinated samples and their TCR usages, epitopes, restricting HLAs and cross-reactive epitopes in microbes other than SARS-CoV-2.

Donor	Clonotype	TRBV	CDR3β	TRBJ	TRAV	CDR3α	TRAJ	S epitope	Restricting HLA	Cross-reactive antigen [species]	Cross-reactive peptide	Post-vaccinated expansion
#4	Pre_5	6-6	CASSYPGGGGSETQYF	2-5	35	CAGVAVQGAQKLVF	54	LLALHRSYLTP$_{241–251}$[a]	DRA-DRB1*14:54	Phosphoribosylformylglycinamidine cyclo-ligase [*Firmicutes bacterium*]	VAEALLAVHRSYLTP$_{220-234}$[b]	No
#4	Pre_7	6-6	CASSYPGGSGGELFF	2-2	21	CAVENSGNTPLVF	29	LLALHRSYLTP$_{241–251}$	DQA1*01:04-DQB1*05:03	Phosphoribosylformylglycinamidine cyclo-ligase [*Firmicutes bacterium*]	VAEALLAVHRSYLTP$_{220-234}$	No
#8	Pre_1	6-2	CASRPNRGRFRGNQPQHF	1-5	23/DV6	CAGEEKETSGSRLTF	58	NCTFEYVSQPFLMDL$_{165–179}$	DRA-DRB1*15:01	Fumarylacetoacetate hydrolase family protein [*Alcaligenes faecalis*] Hypothetical protein [*Planctomycetales bacterium*]	ASLIEYVSQPFLLEP$_{225-239}$ AAGFEYVSQPFSLPL$_{533-547}$	No
#8	Pre_2	6-1	CASIRDRVADTQYF	2-3	30	CGTETTDSWGKLQF	24	RFNGIGVTQNV$_{905–915}$	DQA1*03:02-DQB1*03:03	SEL1-like repeat protein [*Bacteroidaceae bacterium*][c]	LGVYYFNGIGVTQDQ$_{236-250}$	No
#8	Pre_3	27	CATKGEANYGYTF	1-2	12-3	CAMSEMGTGFQKLVF	8	SIVRFPNITNL$_{325–335}$	DRA-DRB1*15:01	LTA synthase family protein [*Dechloromonas denitrificans*]	LPGKSVVRWPNITNL$_{330-344}$	No
#8	Pre_5	5-1	CASSLRTGELFF	2-2	8-1	CAVNGRNTGFQKLVF	8	NFTISVTTEILPVSM$_{717–731}$	DRA-DRB1*09:01	Major capsid protein [*Human papillomavirus 145*] Periplasmic trehalase [*Chlamydiia bacterium*]	NFTISVTTDAGDINE$_{350-364}$ LSTIVTTEILPVDL$_{288-301}$	No
#8	Pre_9	7-2	CASAAGGTGGETQYF	2-5	5	CAETPFLSGTYKYIF	40	YIKWPWYIWLGFIAG$_{1209–1223}$	DRA-DRB5*01:02	Spike glycoprotein [*Human coronavirus HKU1*]	VKWPWYVWLLISFSF$_{1297-1311}$	No
#8	Pre_10	6-6	CASSLGQGIHEQYF	2-7	26-1	CIVERGGSNYKLTF	53	SKRSFIEDLLFNKVT$_{813–827}$	DPA1*01:03-DPB1*04:02	Hypothetical protein, partial [*Acinetobacter baumannii*] Spike protein [*Feline coronavirus*] Spike protein [*Canine coronavirus*]	GKRSAVEDLLFNKVV$_{204-218}$ GKRSAVEDLLFNKVV$_{980-994}$ GKRSAVEDLLFNKVV$_{977-991}$	No
#8	Pre_14	4-3	CASSQRQGAGDTQYF	2-3	19	CALSEAGIQGAQKLVF	54	IDRLITGRLQSLQTY$_{993–1007}$	DQA1*01:03-DQB1*06:01	Excinuclease ABC subunit UvrA [*Lentisphaeria bacterium*]	VDRLITGRLESSRLN$_{208-222}$	No
#8	Pre_15	20-1	CSAKDRIYGYTF	1-2	26-1	CIVRSPSGSARQLTF	22	MIAQYTSALLA$_{869–879}$	DRA-DRB1*15:01	MATE family efflux transporter [*Selenomonas noxia*]	ATIIAQYTSALLALR$_{242-256}$	No
#13	Pre_5	4-3	CASSQVSTGTGITGANVLTF	2-6	5	CARRSSSASKIIF	3	QNVLYENQKLI$_{913–923}$	DRA-DRB5*01:02	Hypothetical protein [*Neobacillus vireti*]	TNVLYENQKLFLNLF$_{169-183}$	No
#13	Pre_8	18	CASSPRAPPYEQYF	2-7	21	CAVRPAGGTGNQFYF	49	DKYFKNHTSPDVDLG$_{1153–1167}$	DRA-DRB1*15:01	Type VI secretion system contractile sheath large subunit [*Salmonella enterica*]	DYYFDHTSPDVDLLG$_{167-181}$	No
#13	Pre_12	4-2	CASSQEGNTEAFF	1-1	20	CGCRGGTSYGKLTF	52	NVTWFHAIHVSGTNG$_{61–75}$	A*02:07	Dihydrofolate synthase [*Actinobaculum sp. 313*]	PQRSFHAIHVTGTNG$_{61-75}$	No
#15	Pre_1	20-1	CSARDLTASAHGYTF	1-2	17	CATDAGQGGKLIF	23	SVTTEILPVSM$_{721–731}$	DQA1*01:03-DQB1*06:01	Hypothetical protein [*Myxococcales bacterium*]	PVTTEILPVSDDPPG$_{525-539}$	No
#15	Pre_2	24-1	CATSDLDQPQHF	1-5	16	CALSGYGSGYSTLTF	11	SVTTEILPVSM$_{721–731}$	DQA1*01:03-DQB1*06:01	Hypothetical protein [*Myxococcales bacterium*]	PVTTEILPVSDDPPG$_{525-539}$	No
#15	Pre_3	6-1	CASDPKNGGEQYF	2-7	29/DV5	CAASVGFGNVLHC	35	FKIYSKHTPIN$_{201–211}$	DRA-DRB5*01:02	Uncharacterized protein APUU_31289S [*Aspergillus puulaauensis*]	CRAAFKLYSKHTPVE$_{123-137}$	No
#15	Pre_4	19	CASGLAGGNTGELFF	2-2	10	CVPSSGGYNKLIF	4	QALNTLVKQLS$_{957–967}$	DRA-DRB1*08:02	4-hydroxybenzoate octaprenyltransferase [*Pseudoduganella dura*]	IQPLNTLVKQLSVAA$_{112-126}$	No
#15	Pre_5	6-5	CASSAGLAGGGNTQYF	2-3	5	CAVISGSARQLTF	22	QALNTLVKQLS$_{957–967}$	DRA-DRB1*08:02	4-hydroxybenzoate octaprenyltransferase [*Pseudoduganella dura*]	IQPLNTLVKQLSVAA$_{112-126}$	No
#15	Pre_6	2	CASVGGNEQFF	2-1	9-2	CALTRFVGGATNKLIF	32	RTFLLKYNENGTITD$_{273–287}$	DRA-DRB1*15:01	Unnamed protein product [*Mytilus edulis*]	NKKLLKYNENGTFIT$_{277-291}$	No
#15	Pre_7	4-1	CASSHDGTPPDTQYF	2-3	29/DV5	CAAYSNYQLIW	33	FKIYSKHTPIN$_{201–211}$	DRA-DRB1*15:01	Uncharacterized protein APUU_31289S [*Aspergillus puulaauensis*]	CRAAFKLYSKHTPVE$_{123-137}$	No
#15	Pre_15	2	CASSETGRGTDTQYF	2-3	9-2	CALYRGTYKYIF	40	LQSLQTYVTQQLIRA$_{1001–1015}$	DRA-DRB1*15:01	Dyp-type peroxidase [*Acinetobacter sp.*]	CTVLQTYVTQQLESV$_{134-148}$	No
#17	Pre_7	6-1	CASSLRGAFGYTF	1-2	35	CAGHLYGGSQGNLIF	42	NCTFEYVSQPFLMDL$_{165–179}$	DPA1*01:03-DPB1*04:02	Fumarylacetoacetate hydrolase family protein [*Alcaligenes faecalis*] Hypothetical protein [*Planctomycetales bacterium*]	ASLIEYVSQPFLLEP$_{225-239}$ AAGFEYVSQPFSLPL$_{533-547}$	No
#17	Pre_8	5-1	CASSLNSGANVLTF	2-6	13-1	CAASIVQDQKLVF	8	LTPTWRVYSTGSNVF$_{629–643}$	DRA-DRB1*08:02	Hypothetical protein [*Novosphingobium chloroacetimidivorans*]	APGTPTWRVYSTART$_{277-291}$	No
#17	Pre_14	5-1	CASSLGAGLYNEQFF	2-1	38-1	CAFINNNAGNMLTF	39	QALNTLVKQLS$_{957–967}$	DRA-DRB1*08:02	4-hydroxybenzoate octaprenyltransferase [*Pseudoduganella dura*]	IQPLNTLVKQLSVAA$_{112-126}$	No
#17	Pre_15	7-2	CASSRTSGGTYEQYF	2-7	25	CAGQNTDKLIF	34	SIVRFPNITNL$_{325–335}$	DRA-DRB1*15:01	LTA synthase family protein [*Dechloromonas denitrificans*]	LPGKSVVRWPNITNL$_{330-344}$	Yes

[a]Number ranges indicate the location of peptides in the proteins.
[b]Amino acids colored red indicate mismatches compared with corresponding S epitopes of Wuhan strain.
[c]Antigen names and peptide sequences in light gray indicate inactive antigens of the corresponding T clonotypes.

Fig. 1

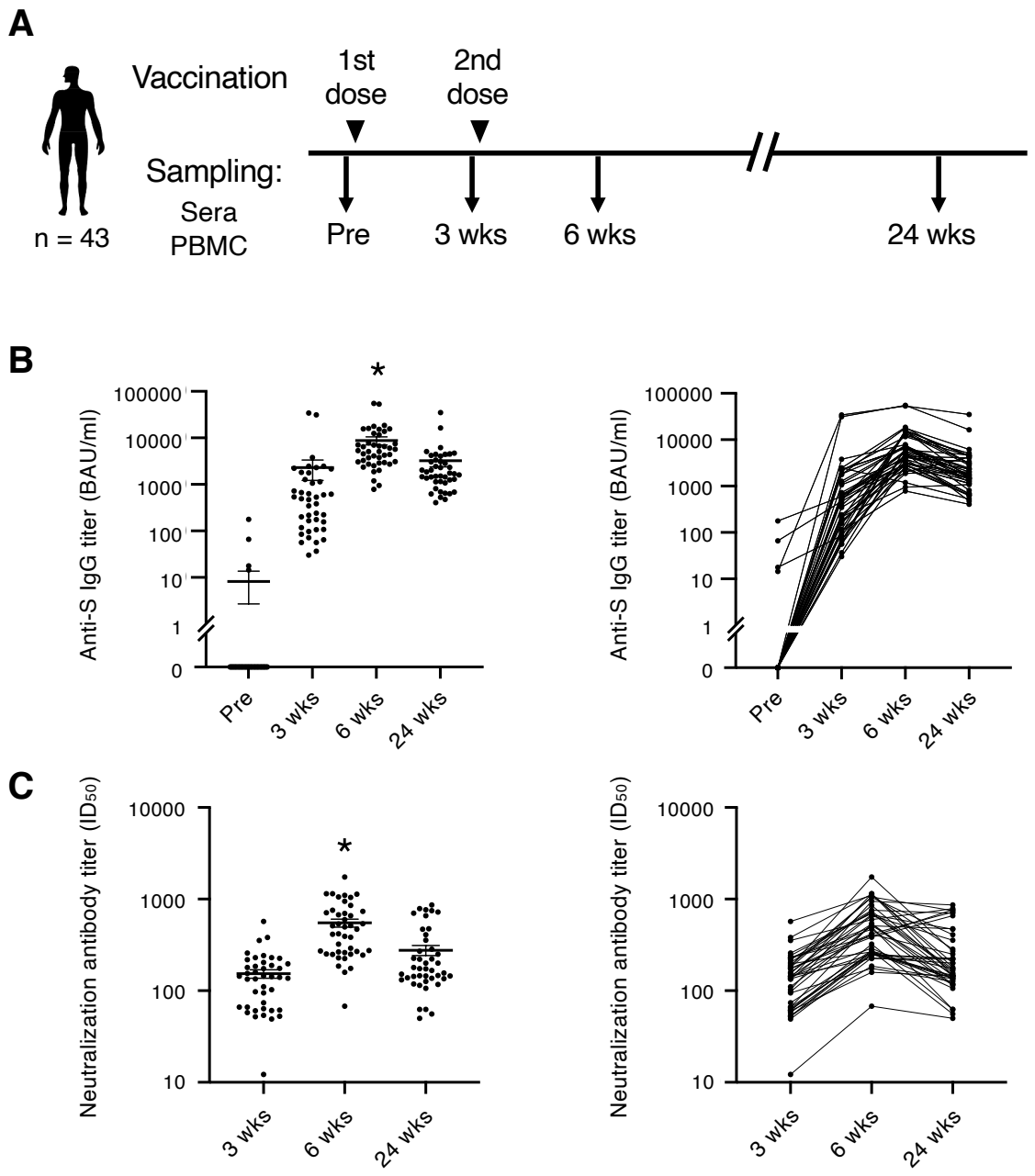

Fig. 1. SARS-CoV-2 mRNA vaccine elicits transient humoral immunity.

(**A**) Vaccination and sampling timeline of blood donors in this study. (**B**) Anti-S IgG titer of serum samples was determined by ELISA. Mean ± SEM (left) and individual data (right) are shown. *, $P < 0.05$ vs. Pre, 3 wks, 24 wks, respectively. (**C**) Neutralization activity (ID50) of serum samples was determined by pseudo-virus assay. Mean ± SEM (left) and individual data (right) are shown. *, $P < 0.05$ vs. Pre, 3 wks, 24 wks, respectively. Wks, weeks.

Fig. 2

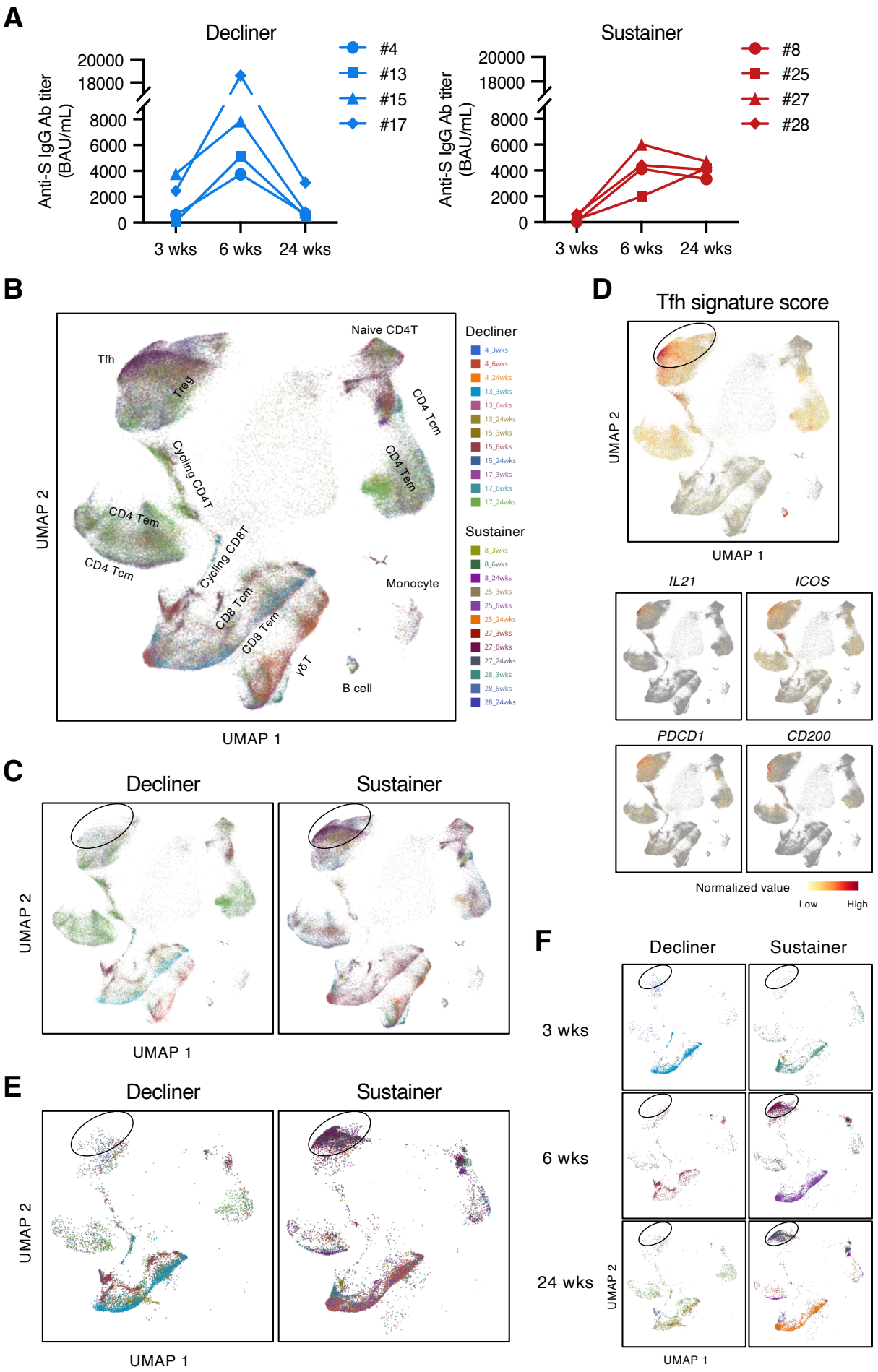
A
Decliner
Sustainer
Anti-S IgG Ab titer (BAU/mL)
20000
18000
8000
6000
4000
2000
0
3 wks
6 wks
24 wks
#4
#13
#15
#17
#8
#25
#27
#28
B
Naive CD4T
Tfh
Treg
CD4 Tcm
CD4 Tem
Cycling CD4T
Cycling CD8T
CD8 Tcm
CD8 Tem
γδT
Monocyte
B cell
UMAP 2
UMAP 1
Decliner
Sustainer
C
Decliner
Sustainer
UMAP 2
UMAP 1
D
Tfh signature score
UMAP 2
UMAP 1
IL21
ICOS
PDCD1
CD200
Normalized value
Low
High
E
Decliner
Sustainer
UMAP 2
UMAP 1
F
Decliner
Sustainer
3 wks
6 wks
24 wks
UMAP 2
UMAP 1

Fig. 2. Antibody sustainers had highly expanded S-reactive Tfh clonotypes.

(**A**) Anti-S IgG titer of serum samples from sustainers and decliners is shown individually. (**B, C, E,** and **F**) UMAP projection of T cells in single-cell analysis of post-vaccinated samples collected from all donors. Each dot corresponds to a single cell and is colored according to the samples from different time points of donors. All samples together with annotated cell types (B), samples grouped by donor type (decliners and sustainers) (C), top 16 expanded clonotypes (16 clonotypes that had the most cell numbers from each donor) grouped by donor type (E), and top 16 expanded clonotypes grouped by time point and donor type (F) are shown. Tcm, central memory T cells; Tem, effector memory T cells; Treg, regulatory T cells; γδT, γδ T cells. (**D**) Tfh signature score and expression levels of the canonical Tfh cell markers, *IL21*, *ICOS*, *PDCD1* and *CD200*, are shown as heat maps in the UMAP plot.

Fig. 3

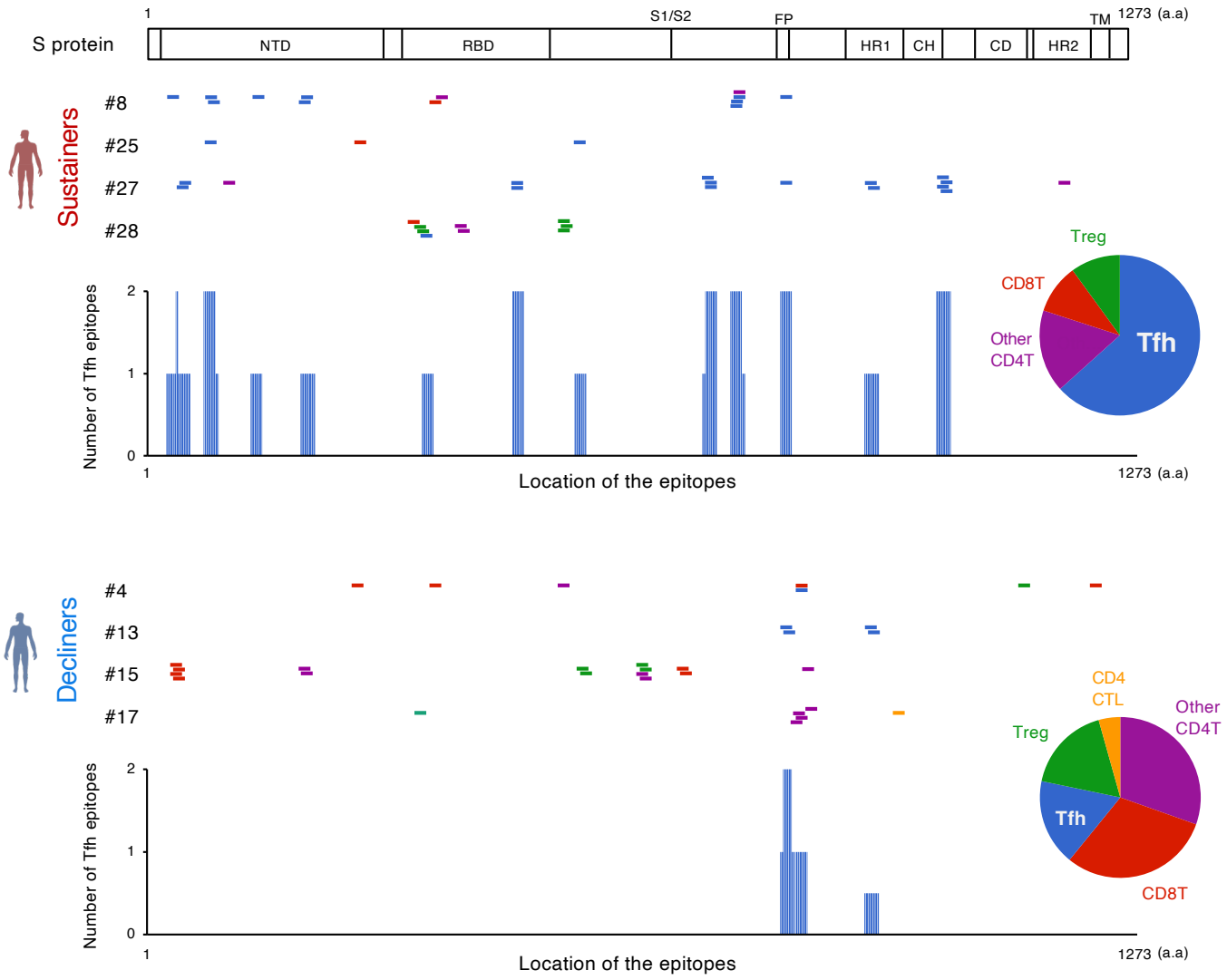

Fig. 3. The location of S epitopes recognized by top expanded T clonotypes from post-vaccination samples.

T cell S epitopes recognized by top expanded TCR clonotypes in post-vaccinated samples from sustainers and decliners are mapped by their locations in S protein. Each short bar indicates a 15-mer peptide that activated the TCRs. Epitopes are shown in different colors according to the subsets of the T cells they activated. Relative frequencies of the T cell subsets are shown in pie charts. Numbers of identified epitopes recognized by a dominant T subset in sustainers (Tfh) are shown in blue bars. NTD, N-terminal domain; RBD, receptor-binding domain; FP, fusion peptide; HR1, heptad repeat 1; CH, central helix; CD, connector domain; HR2, heptad repeat 2; TM, transmembrane domain.

Fig. 4

A

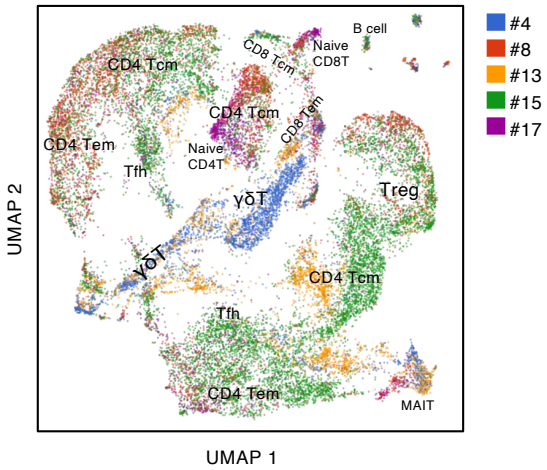

B

Cell number: Min – Max

Donor	Clonotype#	Cell type	Detected cell number					Expansion
			pre	3wks	6wks	24wks	Total	Post(max) /Pre
#13	Post_8	CD4 Tem	239	29	0	27	295	0.12
#15	Pre_1	CD4 Tem	210	0	0	0	210	0.00
#13	Post_1	CD8 Tem	192	2003	43	335	2573	10.43
#13	Pre_2	CD4 Tem	192	0	0	0	192	0.00
#15	Pre_2	CD4 Tem	180	1	21	0	202	0.12
#4	Post_3	CD4 Tem	179	27	1	2	209	0.15
#15	Pre_3	CD4 Tem	178	0	0	13	191	0.07
#15	Pre_4	CD4 Tcm/Treg	174	0	0	0	174	0.00
#13	Post_2	CD8 Tem	165	467	24	920	1576	5.58
#13	Pre_1	MAIT	162	2	0	0	164	0.01
#15	Pre_7	CD4 Tcm	153	0	0	2	155	0.01
#15	Pre_8	CD4 Tem	92	0	0	0	92	0.00
#15	Pre_14	CD4 Tfr	90	0	0	0	90	0.00
#13	Pre_3	CD4 Tcm	87	0	0	0	87	0.00
#15	Pre_5	CD4 Tem	85	0	6	4	95	0.07
#15	Pre_6	CD4 Tem	85	0	0	0	85	0.00
#15	Pre_12	CD4 Tcm/Treg	81	0	0	1	82	0.01
#15	Pre_10	CD4 Tem	77	1	16	0	94	0.21
#4	Pre_1	CD8 Tem	76	4	2	0	82	0.05
#8	Pre_2	CD4 Tem	61	3	1	0	65	0.05
#17	Pre_1	CD4 Treg	61	0	0	0	61	0.00
#8	Pre_4	CD4 Treg	60	7	0	0	67	0.12
#15	Pre_9	CD4 Treg	60	0	0	0	60	0.00
#15		CD4 Treg	60	0	0	0	60	0.00
#8	Pre_1	CD4 Tcm/Treg	60	0	0	0	60	0.00
#15	Pre_15	CD4 Tcm/Treg	58	0	3	0	61	0.05
#15	Pre_13	CD4 Tem	57	0	28	0	85	0.49
#15		CD4 Treg	52	0	13	4	69	0.25
#15		CD4 Treg	52	0	0	0	52	0.00
#15		CD4 Tem	50	0	0	0	50	0.00
#8	Post_1	CD8 Tem	28	164	13	27	232	5.86
#4	Post_1	CD8 Tem	19	17	125	6	167	6.58
#15	Post_3	CD4 CTL	14	14	197	36	261	14.07
#15	Post_8	CD4 CTL	14	6	73	13	106	5.21
#8		CD4 Tfr	9	22	30	0	61	3.33
#17		CD8 Tem	7	16	0	40	63	5.71
#15		CD4 Tfr	7	6	21	20	54	3.00
#17		CD8 Tem	6	0	0	50	56	8.33
#13	Post_3	CD8 Tem	5	54	1	2	62	10.80
#15	Post_2	CD4 CTL/Treg	4	5	217	32	258	54.25
#17	Post_2	CD8 Tem	4	11	4	188	207	47.00
#13	Post_5	CD8 Tem	4	46	3	5	58	11.50
#17		CD8 Tem	2	3	2	58	65	29.00
#8	Post_15	CD4 Treg->CD4 Tcm	2	9	0	41	52	20.50
#13	Post_6	CD8 Tem	1	58	1	12	72	58.00

Fig. 4. Characteristics and dynamics of S-cross-reactive clonotypes.
(**A**) UMAP projection of T cells in single-cell analysis of pre-vaccinated T cells from donors #4, #13, #15, #17, and #8. Each dot corresponds to a single cell and is colored according to the samples from different donors. Annotated cell types are shown. (**B**) Donor, name of reconstituted clonotypes, cell type, number in different time points, and expansion ratio of clonotypes that were found in pre-vaccinated samples and had more than 50 cells in the combined pre- and post-vaccinated sample set. For clonotypes that showed more than one type, the major type is listed in the front. The expansion ratio was calculated using the maximum cell number at post-vaccination points divided by the cell number at the pre-vaccination point of each clonotype. Clonotypes that have an expansion ratio larger than 1 are considered as expanded post-vaccination. Cell numbers at individual time points are shown as heat map. Tfr, follicular regulatory T cells; MAIT, mucosal-associated invariant T cells.

Fig. 5

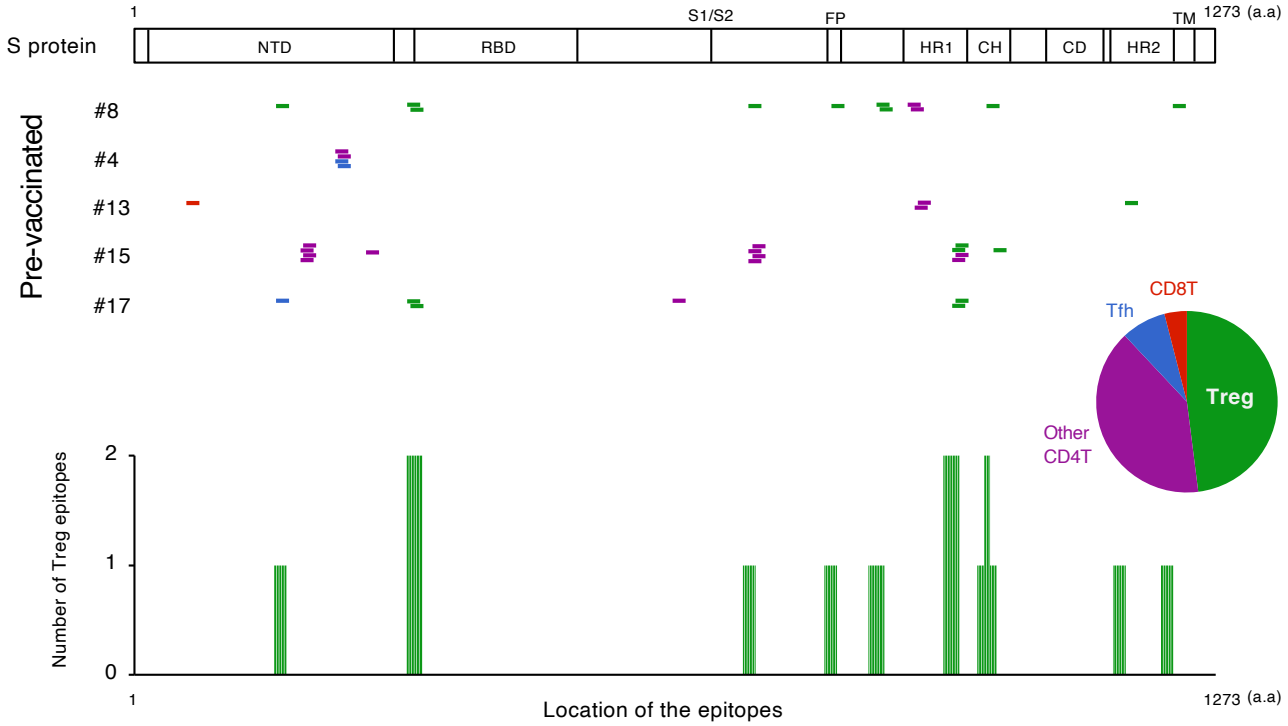

Fig. 5. The location of S epitopes of pre-existing S-reactive T cells.

S epitopes recognized by top expanded TCR clonotypes in pre-vaccinated samples are mapped by their locations in S protein. Each short bar indicates a 15-mer peptide that activated the TCRs. Epitopes are shown in different colors according to the subtypes of the T cells they activated. Relative frequencies of the T cell subtypes from all five donors are shown in the pie chart. Numbers of identified epitopes recognized by a dominant T subset of pre-existing clonotypes (Treg) from all donors are shown in green bars.

Fig. 6

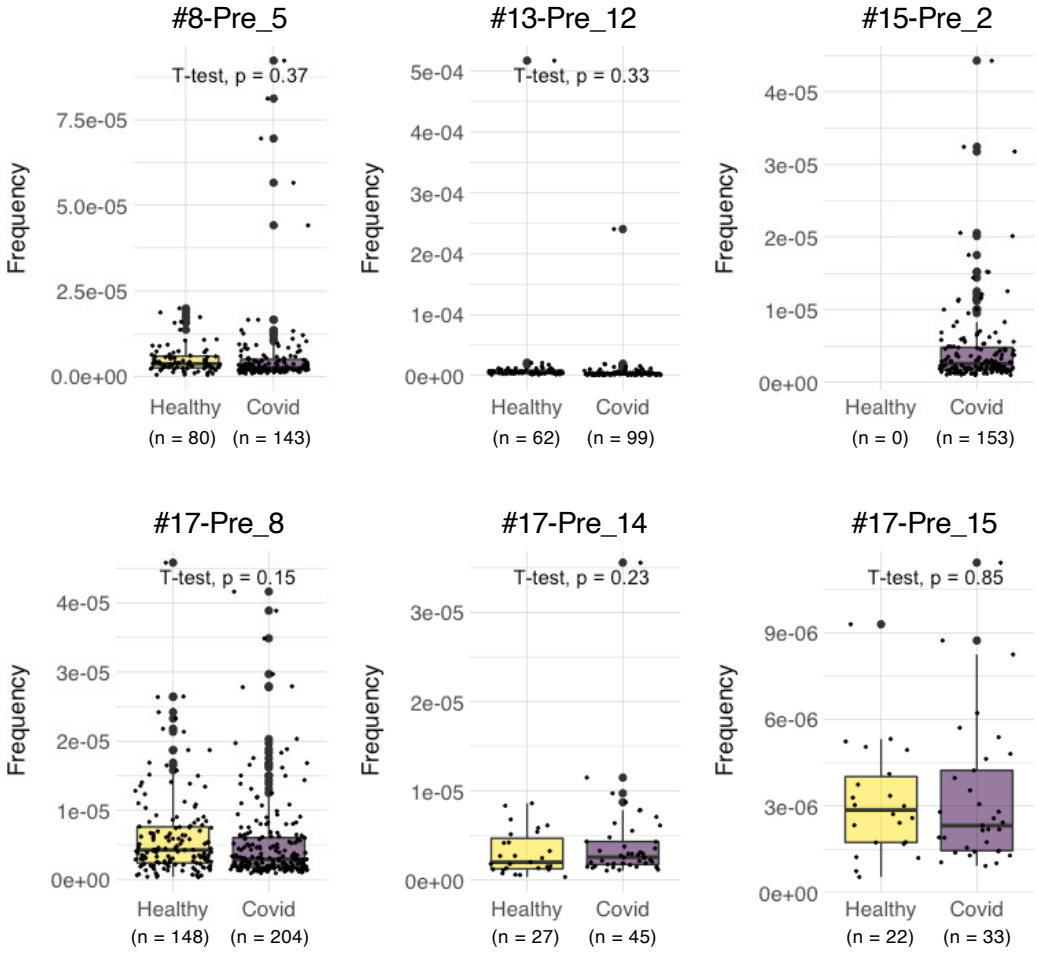

Fig. 6. Frequencies of pre-existing S-reactive clonotypes in the public database of uninfected and infected cohorts.

TCRβ sequences of the top expanded clonotypes in pre-vaccinated samples were investigated in the Adaptive database. Frequencies of detected clonotypes are shown in box plot. Healthy, dataset from 786 healthy donors. COVID, dataset from 1487 COVID-19 patients.